# Supramolecular Copper Phenanthroline Racks: Structures, Mechanistic Insight and Dynamic Nature

**Venkateshwarlu Kalsani,[a] Heinrich Bodenstedt,[a] Dieter Fenske,[b] and Michael Schmittel*[a]**

**Keywords:** Rack / HETPHEN / Self-assembly / Phenanthroline / Dynamics

Herein, we describe the preparation of several dynamic multicomponent supramolecular racks based on copper phenanthroline complexes using the HETPHEN concept (**het**eroleptic bis**phen**anthroline complexes). This approach employs bulky aryl substituents at the bisimine coordination sites to control the coordination equilibrium. The racks were characterised by spectroscopic methods, both in solution ($^1$H NMR, ESI-MS, UV/Vis, vapour pressure osmometry) and in the solid state (X-ray). Ligand exchange studies established the reversible nature of the aggregates, the details of which are vital for the development of higher level multicomponent structures. In this regard, the present rack assemblies contrast to the large multitude of known rack motifs that are almost exclusively built using kinetically inert coordination building blocks.



## Introduction

Metallo-rack structures have a high standing in the burgeoning field of supramolecular chemistry due to their spatially well-defined linear array of metal ions that is attractive for many purposes, such as photoactive and electroactive nanowires.[1] Therefore, facile and quantitative access to rack aggregates is the goal of current research efforts.[1] Racks, however, by their very nature are multi-component structures that are most conveniently assembled under kinetic control, cf. the use of kinetically stable ruthenium coordination complexes,[1b,1c,1e–1g] even at the price of moderate yields. Preparation of rack structures under thermodynamic control is much more a challenge since in a dynamic multitopic aggregation scenario the requested heteroleptic combinations have to compete with homoleptic ones.[1d] Rewardingly, dynamic aggregation should allow for self-repair thus securing the most stable complex in very high yields if sufficient thermodynamic bias is installed.[2] Once the proof of principle is established one is set up to construe dynamic aggregates at surfaces that should be very useful for sensory purposes.[3]

At present, only one strategy is known to construct *dynamic* multicomponent rack structures (Scheme 1; strategy A).[4] Accordingly, ring constraints are utilised to prevent the formation of the homoleptic combination of one of the ligands, e. g. of an endotopic macrocyclic ligand. In combination with another rigid ligand the arrested ligand can combine to a heteroleptic rack-pseudorotaxane motif following the maximum site occupancy principle.[1d] A much easier way to *dynamic* multicomponent racks, however, should emerge from the HETPHEN[5] approach (strategy B). We have recently utilised the HETPHEN concept to establish **het**eroleptic bis**phen**anthroline copper complexes as building blocks for large nanostructures.[6] In our approach, heteroleptic aggregation is driven by steric and electronic factors which do not require an endotopic macrocycle. Instead, steric stoppers are required at the 2,9-positions of one of the bisimine coordination sites to prevent any homoleptic combination with itself. Therefore, in combination with another bisimine ligand only hetero combinations will result. This opens a much more facile way to heteroleptic dynamic aggregation than in previous reports.[7]

We have recently disclosed some preliminary results on dynamic rack structures in the context of our work on supramolecular nanogrids.[8] Herein, we now detail the potential of the HETPHEN[9] concept as a general strategy for the construction of multicomponent dynamic racks, provide structural insight into products and intermediates, and interrogate the dynamic nature of these unique assemblies.

## Results and Discussion

Following the HETPHEN concept two approaches can be explored to prepare dynamic rack-type aggregates (Scheme 2). In both approaches one set of the ligand has to be instructed with the steric stoppers. In **approach I**, the linear bisphenanthroline is loaded with sterically bulky aryl

[a] Center of Micro- and Nanochemistry and Engineering, Organische Chemie I, Universität Siegen,
Adolf-Reichwein-Str., 57068 Siegen, Germany
Fax: +49-271-740-3270
[b] Institut für Anorganische Chemie, Universität Karlsruhe,
Engesserstr. 3045, 76128 Karlsruhe, Germany

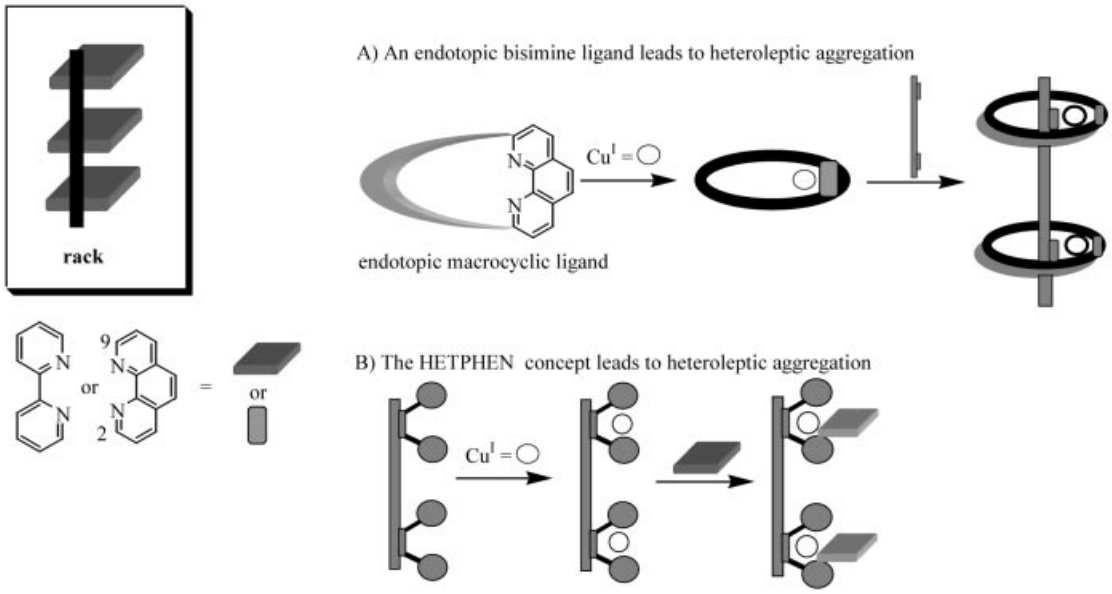


Scheme 1. Strategies to prepare dynamic rack-type motifs.[1d]

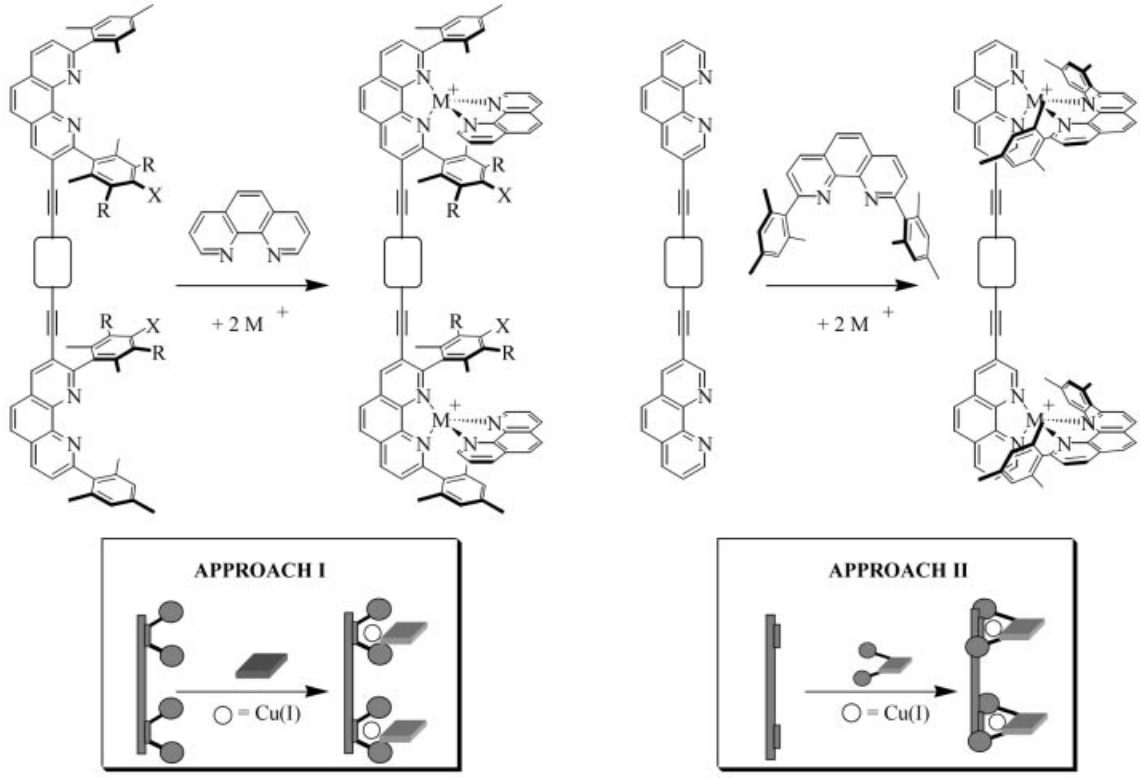


Scheme 2. Two different approaches for constructing dynamic multitopic *rack*-type motifs along the HETPHEN concept (in the bottom: a pictorial cartoon representation of the two approaches).

groups at the 2,9-positions of each phenanthroline site. In contrast, **approach II** makes use of monophenanthrolines that are equipped with the steric stoppers, while the linear bisphenanthroline is devoid of them.

The linear bisphenanthrolines **1a**,[10] **1b**[10] and **2**,[11] as well as the monophenanthrolines **3a**, **3b**,[13] **4a**,[6c] **4b**[12] and **4c**[13] were chosen for this study. Assembly of **1,2** with **3,4** in presence of metal ions of tetrahedral coordination geometry, such as copper(I) or silver(I) ions, is expected to yield the desired dynamic multicomponent racks.

To illustrate the need for control in the formation of dynamic rack assemblies using a coordination approach bisphenanthroline **1a** was treated with **3a** in the presence of $[Cu(MeCN)_4]PF_6$. The desired rack was obtained only as a

  

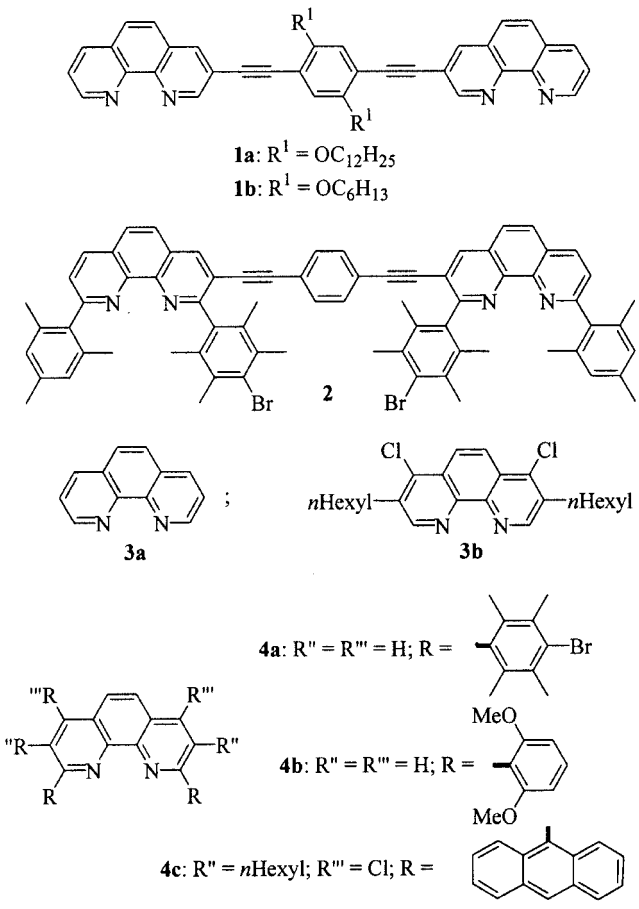


minor component as evidenced by ESI-MS and $^1$H NMR spectroscopy. Rather, a complex mixture formed showing signals corresponding to the triangular-grid and signals corresponding to the homoleptic complex of **3a** as depicted in Scheme 3. $^1$H NMR showed various sets of signals which arise from the resulting different aggregates. It is clear from the above experiment that cooperativity[7] can not be used solely to build dynamic heteroleptic aggregates.

## Approach I

As discussed above, approach I uses a bisphenanthroline that has steric stoppers (as in ligand **2**) in combination with any phenanthroline with no steric stoppers at 2,9-positions (i.e. **3a**–**3b**). The combination of these two building blocks and $Cu^I$ salt should result in heteroleptic racks.[8] Indeed, upon addition of $[Cu(MeCN)_4]PF_6$ to a dichloromethane solution of **2** and **3** the rack structures **R1,R2** were exclusively furnished as demonstrated by $^1$H NMR, $^{13}$C NMR, ESI-MS, and elemental analysis.

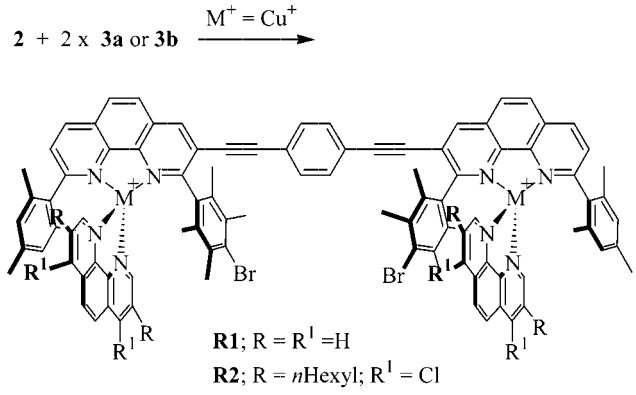


**Mechanistic Tests on the Formation of $[Cu_2(2)]^{2+}$.** Rack **R1** $[Cu_2(\mathbf{2})(\mathbf{3a})_2]^{2+}$ was selected as a model system and its formation systematically investigated using a variety of spectroscopic techniques (by, $^1$H NMR, ESI-MS and spectrophotometric titrations). Treatment of ligand **2** with 2 equiv. of $[Cu(MeCN)_4]PF_6$ resulted in a yellow solution, the analysis of which by UV/Vis (absence of a MLCT band at 430–550 nm of a $[Cu(phenanthroline)_2]^+$ complex), ESI-MS and $^1$H NMR suggested the formation of $[Cu_2(\mathbf{2})(MeCN)_2]^{2+}$ as the sole species. As expected, ligand **2** acts as a **HETPHEN** ligand that is not able to self-assemble to a homoleptic grid.

Progressive addition of $[Cu(MeCN)_4]PF_6$ to **2** (in dichloromethane) provided valuable information about the intermediates as they could be readily detected by ESI-MS, $^1$H NMR, and UV/Vis spectroscopy. In the $^1$H NMR spectrum, for example, the mesityl protons Mes-*H* can be used as a diagnostic marker to assign the composition of the intermediate species present in the equilibrium. Addition of $Cu^I$ salt to **2** in dichloromethane resulted in two new sets of signals, one of which built up at the initial stage of the titration and disappeared as the titration proceeded. The first set of signals, formed during addition of the first equiv. of $Cu^I$ salt, was assigned to $[Cu(\mathbf{2})(MeCN)]^+$. After addition of 2 equiv. of $Cu^I$ salt a single set of signals resulted which could be readily assigned to $[Cu_2(\mathbf{2})(MeCN)_2]^{2+}$. Im-

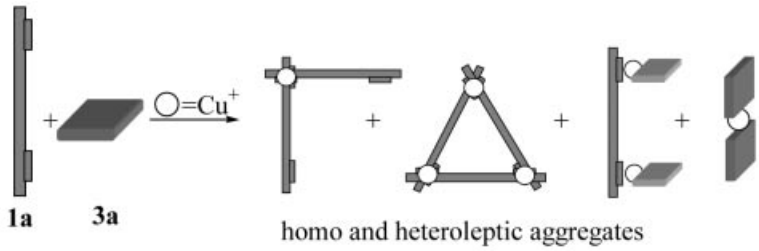


Scheme 3. Cartoon representation of the self-assembly of linear bisphenanthrolines and monophenanthrolines that are not instructed along the HETPHEN concept.

  

portantly, during the whole process no signals were detectable at 5–6 ppm, which is considered to be a characteristic range for mesityl protons of a $[Cu(phenanthroline)_2]^+$ complex.[9] ESI-MS titration results further supported the above assignments.

The UV/Vis titration revealed the absence of a band at ca. 500 nm, indicating that formation of a $[Cu(phenanthroline)_2]^+$ complex with its characteristic MLCT had not occurred. These results indicate that in line with the behaviour of monophenanthroline analogs[9] ligand **2** has been successfully instructed not to assemble with itself.

Most convincingly the structure of $[Cu_2(\mathbf{2})(MeCN)_2]^{2+}$ was supported by a single crystal structure analysis (Figure 1). It is worthwhile to note that, though the present system is a simple one, the solid state characterisation of such an intermediate in a coordination equilibrium is quite unique. $[Cu_2(\mathbf{2})(MeCN)_2]^{2+}$ has neither a *syn* or *anti* conformation with regard to the two phenanthroline binding sites. Instead, the two sites comprise a dihedral angle of ca. 122 deg. Each copper(I) center is coordinated to one phenanthroline and a single acetonitrile molecule. The average Cu–$N_{phen}$ bond length is 204 ± 3 pm, while the Cu–$N_{MeCN}$ distance is much shorter with 186 pm (Table 1). In conclusion, the solid-state structure along with the $^1$H NMR, ESI-MS and UV/Vis studies proves unequivocally that the HETPHEN concept allows to control the coordination equilibrium of specially designed phenanthroline ligands and to prevent formation of any bishomoleptic complex formation.

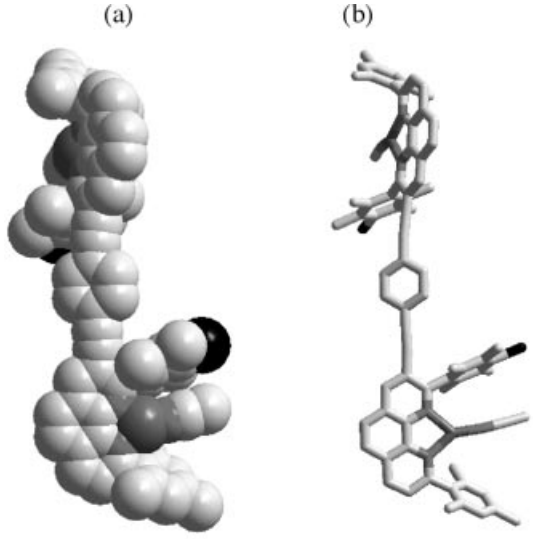


Figure 1. a) Space filling and b) stick representation of the crystal structure of $[Cu_2(\mathbf{2})(MeCN)_2]^{2+}$.

**Mechanistic Tests on Formation of $[Cu_2(2)(3a)_2]^{2+}$.** Upon addition of a second phenanthroline, such as **3a** or **3b**, to the intermediate $[Cu_2(\mathbf{2})(MeCN)_2]^{2+}$ in dichloromethane, the racks **R1** or **R2** were afforded in basically quantitative yield as evidenced by $^1$H-NMR and ESI-MS. For example, in case of **R1** ESI-MS showed the presence of one single species at $m/z$ = 814.5 which corresponds to $\mathbf{R1}^{2+}$. Equally, the $^1$H-NMR illustrated the presence of a single symmetric species (Figure 2). The distinct high field shifts for the mesitylene protons (6.76 to 5.89 ppm) of **2** clearly indicated the formation of a bisheteroleptic complex.

Table 1. Selected Bond Lengths [Å] and Angles [°] for $[Cu_2(\mathbf{2})(MeCN)_2]^{2+}$.

| Bond | Length [Å] | Angle | Angle [°] |
|---|---|---|---|
| N1–Cu1 | 2.016(17) | N1–Cu1–N5 | 146.14(1) |
| N2–Cu1 | 2.050(9) | N2–Cu1–N5 | 130.10(1) |
| N5–Cu1 | 1.856(18) | N2–Cu1–N1 | 82.91(2) |
| N3–Cu2 | 2.071(7) | N3–Cu2–N6 | 131.88(1) |
| N4–Cu2 | 2.017(21) | N4–Cu2–N6 | 142.61(2) |
| N6–Cu2 | 1.861(20) | N3–Cu2–N4 | 82.54(2) |

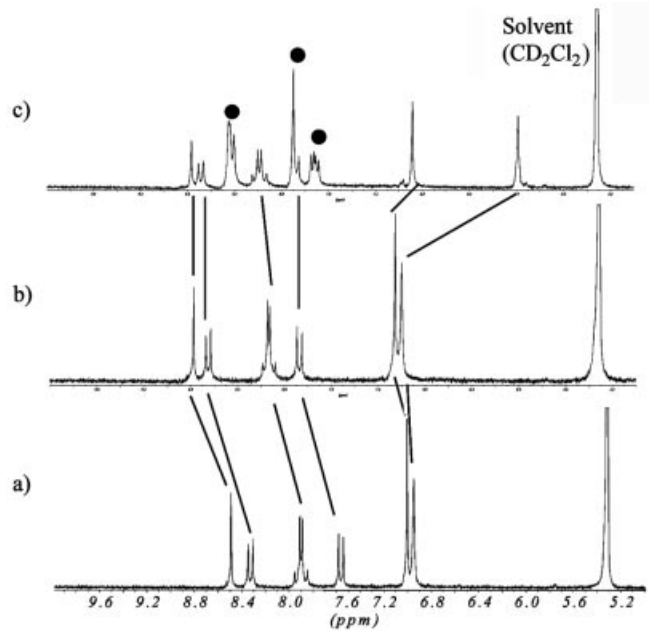


Figure 2. $^1$H NMR changes in the aromatic region of **2** upon complexation with **3a**. a) free **2**; b) $[Cu_2(\mathbf{2})(MeCN)_2]^{2+}$; c) $[Cu_2(\mathbf{2})(\mathbf{3a})_2]^{2+}$. Signals in Figure **c** being marked by filled spheres belong to phenanthroline (**3a**) protons.

For further understanding, a titration was performed, in which **3a** was added to a dichloromethane solution of $[Cu_2(\mathbf{2})(MeCN)_2]^{2+}$ leading to pronounced changes in the $^1$H NMR spectra. With the titration proceeding, two different sets of signals evolved for the mesityl protons that were readily assigned to $[Cu(\mathbf{2})(\mathbf{3a})]^+$ and $[Cu_2(\mathbf{2})(\mathbf{3a})_2]^{2+}$ using parallel ESI-MS results. While ESI-MS and $^1$H NMR titrations proposed a qualitative picture of the mechanism of the self-assembly process, a UV/Vis titration was undertaken to determine the binding constants. It was performed by titrating **2** ($1.2\,10^{-6}$ M) and **3a** ($2.4\,10^{-6}$ M) with aliquot amounts of $Cu^I$ solution in 20 additions (total 4 equiv. of $Cu^+$). Figure 3 displays the UV/Vis changes upon $Cu^I$ salt addition showing the emerging MLCT transition at ca. 490 nm that is responsible for the red color. As shown in Scheme 4 a two step pathway seems most reasonable for the rack assembly process: it starts out with the formation of $[Cu(\mathbf{2})(\mathbf{3a})]^+$ taking up one more ligand **3a** and $Cu^I$ to furnish the $[Cu_2(\mathbf{2})(\mathbf{3a})_2]^{2+}$ complex. The structure of

  

$[Cu_2(\mathbf{2})(\mathbf{3a})_2]^{2+}$ was confirmed by its single crystal analysis.[8] Upon fitting this model with UV/Vis data using the SPECFIT program[14] binding constants could readily be extracted for complexes $[Cu(\mathbf{2})(\mathbf{3a})]^+$ (log $K_{111}$ = 11.6) and $[Cu_2(\mathbf{2})(\mathbf{3a})_2]^{2+}$ (log $\beta_{212}$ = 23.1). Models that did not fit were rejected.

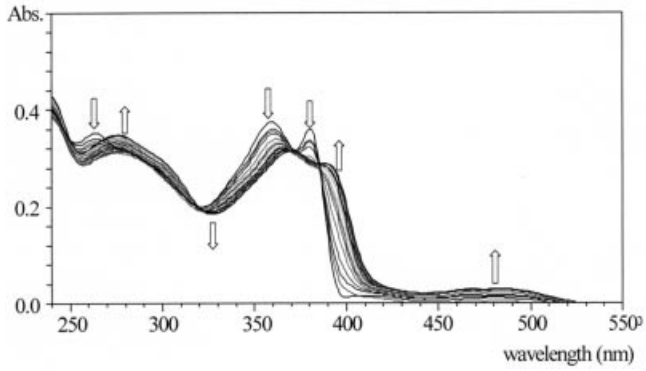


Figure 3. Spectrophotometric titration of **2** and 1,10-phenanthroline (**3a**) by aliquot amounts of $Cu^I$ salt in 20 additions. Solvent: dichloromethane. $T$ = 25(1) °C. [**2**] = $1.20\times10^{-6}$ M and [**3a**] = $2.40\times10^{-6}$ M.

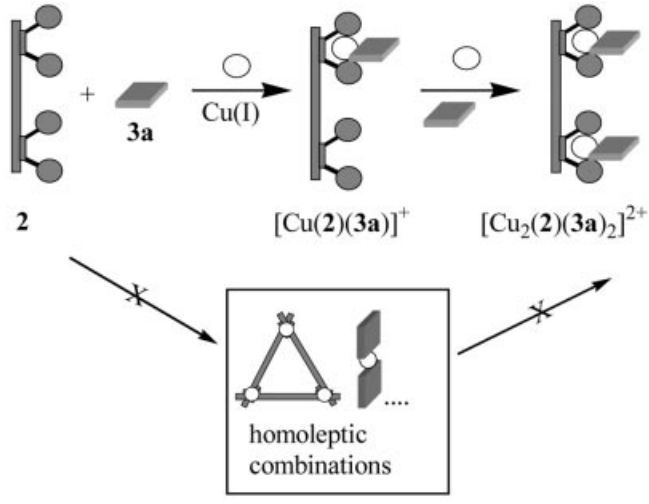


Scheme 4. Self-assembly path for **R1**.

## Approach II

As suggested above, rack motifs should also be accessible by approach II. **4a**–**c** were designed according to the HETPHEN strategy, i.e. the 2,9-positions of all monophenanthrolines were loaded with steric stoppers while bisphenanthroline **1a** and **1b** were devoid of this element. Notably, racks **R3**–**R5** were readily afforded upon reacting **1a** with **4a**–**c** in presence of $[Cu(MeCN)_4]PF_6$ (Scheme 5). Similarly, **R6** was obtained by reacting **1b**, **4a** and $Cu^I$ salt in dichloromethane (1:2:2 equiv.). All spectroscopic data was consistent with the proposed composition (see experimental section).

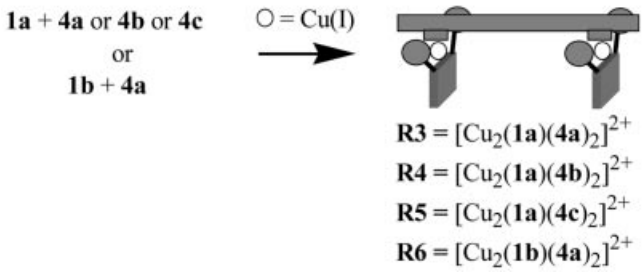


Scheme 5.

Apart from conventional characterisation techniques ($^1$H NMR, ESI-MS, UV/Vis, and elemental analysis), vapour pressure osmometry (VPO) was applied to characterise **R3** as one of the aggregates. VPO is a very useful method to analyse self assembled systems even if they are dynamic;[15] unfortunately, this technique has not been utilised frequently. For **R3** VPO provided a molar mass of 2417 Da, which is in excellent agreement (–2%) with the mass obtained from ESI-MS (2473). The characterisation of even larger dynamic structures by VPO is currently under investigation in our laboratory.

The structure of **R6** was solved by single-crystal X-ray analysis. The stick representation of the solid-state structure of **R6** is depicted in Figure 4. Unlike a previous structure[8] this rack has some deviation from prefect *transoid* conformation. Each copper(I) centre exhibits a pseudotetrahedral coordination geometry (N1–Cu1–N4 108.4°, N2–Cu1–N3 125.0°, N5–Cu2–N8 123.1°, N6–Cu2–N7 120.1°) and finds itself encapsulated by two bromoduryl rings of the bisphenanthroline (Table 2). The duryl groups of **4a** and the phen-

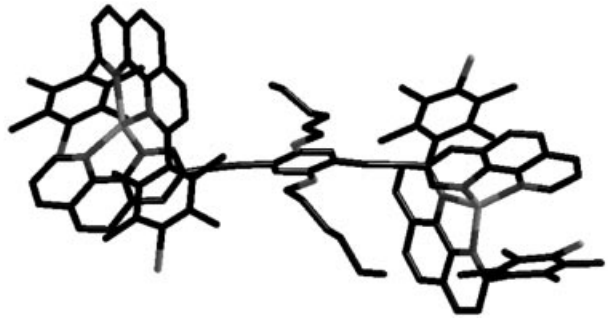

Figure 4. Single crystal structure of **R6**; stick representation.

Table 2. Selected bond lengths [Å] and angles [°] for **R6**.

| Bond | Length [Å] | Angle | Angle (in degrees) |
|---|---|---|---|
| Cu1–N4 | 1.998 | N4–Cu1–N2 | 131.9(4) |
| Cu1–N3 | 2.038 | N4–Cu1–N3 | 81.5(4) |
| Cu1–N2 | 2.063 | N2–Cu1–N3 | 125.0(4) |
| Cu1–N1 | 2.092 | N4–Cu1–N1 | 108.0(4) |
| N2–Cu1–N1 | 81.0(5) | | |
| N3–Cu1–N1 | 135.0(4) | | |
| Cu2–N8 | 2.062 | N7–Cu2–N8 | 80.0(5) |
| Cu2–N7 | 2.006 | N7–Cu2–N6 | 119.5(4) |
| Cu2–N5 | 2.029 | N8–Cu2–N6 | 127.5(4) |
| Cu2–N6 | 2.069 | N7–Cu2–N5 | 129.0(4) |
| | | N8–Cu2–N5 | 123.0(4) |
| | | N6–Cu2–N5 | 82.5(4) |

  

anthroline plane of the second ligand **1b** are oriented face-to-face separated by 3.5 Å, suggesting π-stacking.

### Dynamic Nature of Rack Motifs

The dynamic nature of the rack motifs was tested by an exchange experiment.[16] Specifically, we monitored the ligand exchange between **R3** and **R4** by using ESI-MS, with ligand **1a** being common in both **R3** and **R4** (Scheme 6). $^1$H NMR experiments on the **R3** + **R4** ⇋ **R7** equilibration could not be performed due to signal overlap. However, the present example was studied by ESI-MS furnishing sensible insight into the dynamics of such aggregates. Such investigations are very informative when NMR application is limited.

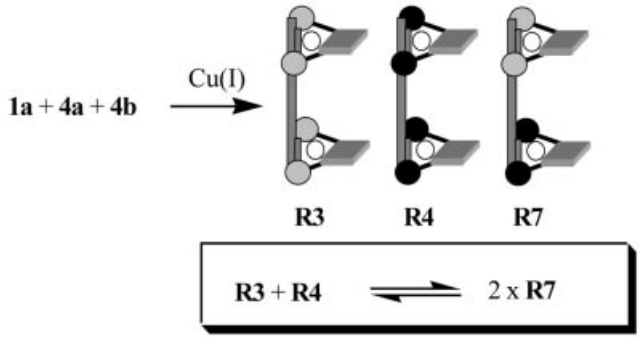


Scheme 6. Cartoon representation of ligand exchange equilibrium in solution after mixing **R3** and **R4**.

**R3** and **R4** in dry dichloromethane were reacted in a 1:1 stoichiometric ratio. The ligand exchange process was observed readily (within ca. 5 min) by ESI-MS exhibiting signals corresponding to a mixture of the three racks **R3**, **R4** and **R7** in a %-ratio of 55, 55 and 100, respectively. This ratio did not change after longer times, indicating that equilibrium had been established at room temp. within less than 5 min (Figure 5). Analgous results were obtained when the racks were generated in one pot by reacting **1a**, **4a** and **4b** in presence of Cu$^{I}$ salt. Isotopic distributions of **R3**, **R4** and **R7** were in excellent agreement with the calculated ones.

The composition was further confirmed by collisional fragmentation experiments. At higher voltages and temperature the ESI-MS is dominated by [Cu(**4a** or **4b**)(**1a**)]$^+$

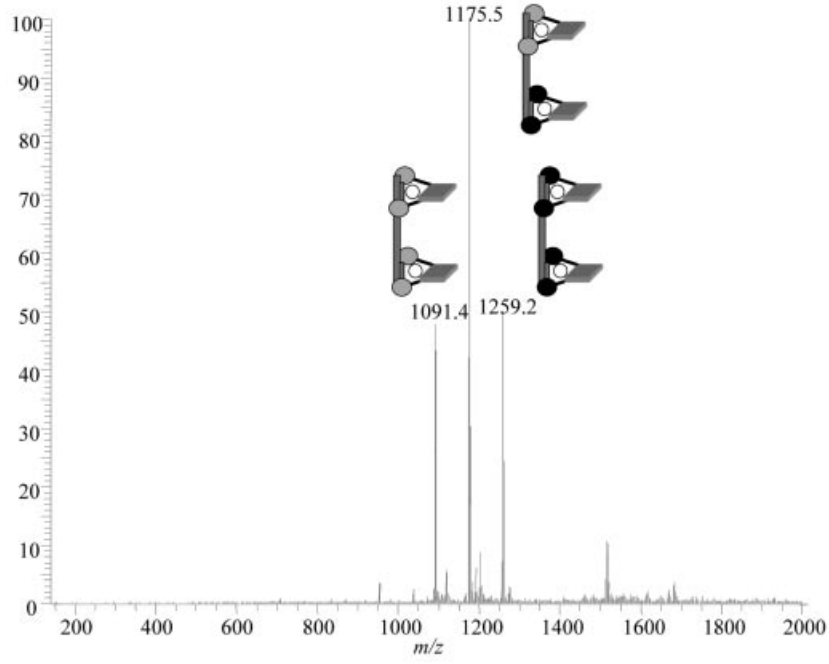


Figure 5. ESI-MS of the reaction mixture obtained when **1a**, **4a**, **4b** are treated with Cu$^{I}$ salt in dichloromethane.

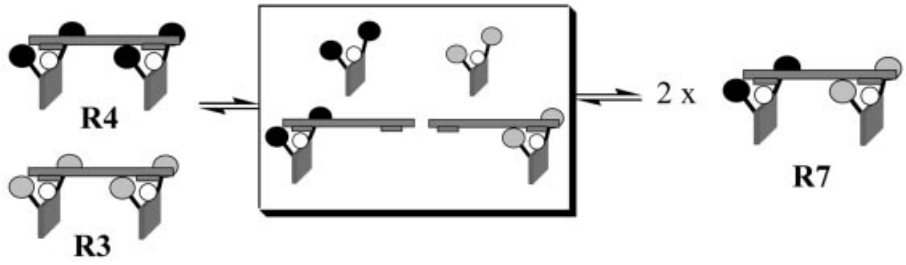


Scheme 7. Mechanism of the dynamic ligand exchange in the interconversion of racks.

  

and [Cu(**4a** or **4b**)]$^+$ as fragments. It is interesting to note that a similar behaviour was observed for all rack structures, i.e. it is always the sterically loaded ligand that is bound to the metal ion in fragmentation processes. Presumably due to cation-π interactions between $Cu^+$ and 2,9-aryl groups complexes [Cu(**4a** or **4b**)]$^+$ are more stable than other combinations. These findings were corroborated through collisional fragmentation experiments of **R3**, **R4** and **R7**. For example, fragmentation of **R4** produced signals corresponding to the [Cu(**4b**)(**1a**)]$^+$ and [Cu(**4b**)]$^+$ species. If we translate these ESI-MS results onto the equilibration process in solution then it is reasonable to assume that in the dynamic ligand exchange any dissociation occurs with the metal ions attached to the sterically shielded HETPHEN ligands (Scheme 7).

## Conclusions

In summary, the HETPHEN concept proves its value for the clean preparation of racks **R1**–**R6** from various bisphenanthrolines and monophenanthrolines in presence of $Cu^+$. X-ray and solution spectroscopic data, including ESI-MS, UV/Vis titrations and vapour pressure osmometry, disclose a clear picture of the self-assembly pathway and the products. Accordingly, ligands shielded along the HETPHEN concept (**2** and **4**) bind strongly to the copper ions but are instructed not to undergo self-association to homoleptic complexes. In combination with unshielded ligands **1** and **3** racks **R1**–**R6** are formed in a stepwise manner. Racks **R1**–**R6** are dynamic in nature as demonstrated in exchange processes at room temperature. Since $Cu^I$-based bisphenanthroline complexes are potential photoactive devices,[17] the present results should open an easy venue to diverse functional aggregates. Studies are in progress to install multi-functionalities into these rack motifs and to study their properties as a function of the dynamic behaviour.

## Experimental Section

Ligands, **1a**,[11] **1b**,[11] **2**,[11] **3b**,[13] **4a**,[6c] **4b**[12] and **4c**[13] were prepared according to known procedures. $^1$H NMR and $^{13}$C NMR were measured on a Bruker AC 200 (200 MHz) or Bruker AC 400 (400 MHz). All $^1$H NMR measurements were carried at room temperature in [$D_2$]dichloromethane. ESI-MS spectra were measured on a LCQ Deca Thermo Quest. Typically, each time 25 scans were accumulated for one spectrum. UV/Vis spectra were recorded on a Tidas II spectrophotometer using dichloromethane as the solvent.

Spectrophotometric titrations: Equilibrium constants of the complexes were determined in dichloromethane. Ligands 2 and 3a were titrated with aliquot amounts of a stock solution of copper(I) tetrakisacetonitrile hexafluorophosphate. All stock solutions were prepared by careful weighing (microgram scale) on an analytical balance. Absorption spectra were recorded at 25.0±(0.1) °C. Since the formation is instantaneous as evidenced by proton NMR, ESI-MS analysis and visible colour changes, the solutions were immediately analysed spectroscopically to avoid problems with the volatile solvent. The wavelength region from 240 nm to 600 nm was taken into account. Two equivalents (total) of metal salt in dichloromethane solution were added in 20 portions. The entire data sets comprising absorbances measured with one nanometer resolution were decomposed in their principal components by factor analysis. Subsequently, formation constants and their standard deviations were calculated by using the SPECFIT[14] program. Binding constants were determined from two independent titrations.

**Vapor-Pressure Osmometry:** The instrument (EuroOsmo 7000) was operated at 27 °C, dry dichloromethane was used as solvent. Calibration was performed by using tetrabutylammonium hexafluorophosphate as standard.

**General Procedure for the Preparation of Racks R1–R6:** Racks **R1**–**6** were prepared by mixing **1** (or **2**) and **3** (or **4**) with [Cu(MeCN)$_4$]$PF_6$ (1:2:2 equiv., respectively) in dichloromethane. The resulting dark red compound was analysed without any further purification by ESI-MS, $^1$H NMR, COSY, $^{13}$C NMR, IR and elemental analysis.

**[$Cu_2$(2)(3a)$_2$]($PF_6$)$_2$ (R1):** M.p. > 300 °C. $^1$H NMR ($CD_2Cl_2$, 400 MHz): $\delta$ = 8.81 (s, 2 H, phen), 8.73 (d, $J$ = 8.1 Hz, 2 H, phen), 8.40–8.50 (m, 8 H, phen), 8.23 (dd, 4 H, $J$ = 8.1, $J$ = 4.0 Hz, phen), 7.94 (s, 4 H, phen), 7.92 (d, $J$ = 8.1 Hz, 2 H, phen), 7.75 (m, 4 H, phen), 6.93 (s, 4 H, phenyl), 6.03 (s, 4 H, mes), 1.81 (s, 12 H, $CH_3$), 1.59 (s, 12 H, $CH_3$), 1.57 (s, 18 H, $CH_3$). $^{13}$C NMR ($CD_2Cl_2$, 100 MHz): $\delta$ = 161.3, 159.9, 148.1, 144.3, 143.2, 142.9, 139.9, 139.1, 138.2, 138.1, 136.9, 135.0, 134.1, 133.6, 132.5, 131.9, 129.2, 129.1, 128.7, 128.1, 127.9, 127.6, 127.3, 125.1, 122.9, 122.5, 117.5, 117.1 (arom.); 96.7, 87.7 (ethynyl); 20.6, 20.3 (2C), 18.5 (aliph.). IR (KBr): $\tilde{\nu}$ = 3411, 3057, 2919, 2209 (νC≡C), 1718, 1655, 1636, 1509, 1438, 1381, 1083, 856, 729, 550. ESI-MS: calcd. for $C_{96}H_{76}Br_2Cu_2N_8^{2+}$ [$M^{2+}$]: *m*/*z* 814.3, found: *m*/*z* 814.5. $C_{96}H_{76}Br_2Cu_2N_8{\times}2\,PF_6{\times}2\,H_2O$ (1954.54): C 58.99, H 4.13, N 5.73; found: C 58.95, H 4.01, N 5.84.

**[$Cu_2$(2)(3b)$_2$]($PF_6$)$_2$ (R2):** M.p. > 300 °C. $^1$H NMR ($CD_2Cl_2$, 200 MHz): $\delta$ = 8.78 (s, 2 H, phen), 8.74 (d, 2 H, $J$ = 8.4 Hz, phen), 8.20–8.36 (m, 10 H, phen), 7.91 (d, 2 H, $J$ = 7.9 Hz, phen), 7.53 (s, 2 H, phen), 6.84 (s, 4 H, phenyl), 6.15 (s, 4 H, mes), 2.91–3.01 (m, 8 H, hexyl), 1.83 (s, 12 H, benzyl), 1.56 –1.65(m, 30 H, benzyl), 1.33 (s, 32 H, aliph.), 0.86 (s, 12 H, aliph.). $^{13}$C NMR ($CD_2Cl_2$, 100 MHz): $\delta$ = 161.0, 159.9, 149.2, 144.1, 142.7, 142.3, 142.1, 140.5, 139.7, 138.6, 138.4, 138.1, 138.0, 137.7, 134.9, 133.4, 132.3, 131.8, 129.9, 129.1, 128.8, 128.1, 127.6, 127.3, 126.8, 124.4, 122.8, 122.5 (arom.); 96.7, 87.5 (ethynyl); 32.1, 31.8, 30.0, 29.4, 22.9, 20.6, 20.3, 20.1, 18.4, 14.2 (aliph.). IR (KBr): $\tilde{\nu}$ = 3439, 2926, 2857, 2212 (νC≡C), 1617, 1571, 1492, 1459, 1421, 1371, 1084, 842, 727, 635, 558. ESI-MS: calcd. for $C_{120}H_{120}Br_2Cl_2Cu_2N_8^{2+}$ [$M^{2+}$]: *m*/*z* 1051.5, found: *m*/*z* 1052.3. $C_{120}H_{124}Br_2Cl_4Cu_2N_8O_2{\times}2\,PF_6{\times}2\,H_2O$ (2428.96): C 59.34, H 5.15, N 4.61; found: C 59.13, H 4.95, N 4.51.

**[$Cu_2$(1a)(4a)$_2$]($PF_6$)$_2$ (R3):** M.p. > 300 °C. $^1$H NMR ($CD_2Cl_2$, 200 MHz): $\delta$ = 8.51 (d, $J$ = 8.6 Hz, 4 H, phen), 8.43 (m, 8 H, phen), 7.99 (s, 4 H, phen), 7.91 (m, 8 H, phen), 7.75 (dd, $J$ = 8.9, $J$ = 4.9 Hz, 2 H, phen), 7.06 (s, 2 H, phenyl), 4.01 (t, $J$ = 5.5 Hz, 4 H, -$OCH_2$-), 1.70 (m, 40 H, benzyl), 1.53 (s, 14 H, benzyl and aliph.), 1.17–1.22 (m, 34 H, aliph.), 0.86 (t, $J$ = 5.5 Hz, 6 H, aliph.). $^{13}$C NMR ($CD_2Cl_2$, 100 MHz): $\delta$ = 160.1, 154.2, 149.3, 148.6, 145.1, 143.3, 142.1, 141.7, 138.9, 138.4, 136.3, 134.1, 133.6, 133.1, 130.4, 129.7, 129.1, 127.5, 126.8, 126.4, 123.4, 123.1, 118.5, 113.1 (arom.); 93.5, 91.4 (ethynyl); 33.4, 29.7 (2C), 30.1 (2C), 30.9 (2C), 26.5, 23.4, 21.1 (2C), 20.4, 19.1 (2C), 14.5 (aliph.). IR (KBr): $\tilde{\nu}$ = 3444, 2852, 2208 (νC≡C), 1618, 1579, 1498, 1459, 1426, 1388, 1221, 1164,

  

1018, 936, 872, 843, 724, 632, 558. ESI-MS: calcd. for $C_{122}H_{126}Br_4Cu_2N_8O_2^{2+}$ [$M^{2+}$]: *m/z* 1091.5, found: *m/z* 1090.7. $C_{122}H_{128}Br_4Cu_2N_8O_3\times2PF_6\times H_2O$ (2491.01): C 58.82, H 5.18, N 4.50; found: C 58.62, H 5.29, N 4.34.

**[$Cu_2$(1a)(4b)$_2$]($PF_6$)$_2$ (R4):** M.p. > 300 °C. $^1$H NMR ($CD_2Cl_2$, 200 MHz): $\delta$ = 8.62 (s, 2 H, phen), 8.58 (s, 4 H, phen), 8.39–8.8.51 (m, 6 H, phen), 8.15 (s, 4 H, phen), 7.18–7.96 (m, 8 H, phen), 7.70 (dd, *J* = 8.9, *J* = 4.1 Hz, 2 H, phen), 7.01 (s, 2 H, phenyl), 6.45 (t, 4 H, *J* = 8.4 Hz, phenyl), 5.71 (m, 8 H, phenyl), 3.95 (t, *J* = 6.7 Hz, 4 H, -$OCH_2$-), 3.30 (s, 12 H, methoxy), 3.26 (s, 12 H, methoxy), 1.70–1.77 (m, 4 H, aliph.), 1.15–140 (m, 36 H, aliph.), 0.86 (t, *J* = 5.9 Hz, 6 H, aliph.). $^{13}$C NMR ($CD_2Cl_2$, 100 MHz): $\delta$ = 160.4, 159.3, 148.6, 143.5, 141.7, 141.5, 139.9, 139.2, 138.1, 137.9, 137.4, 137.1, 134.3, 132.8, 131.7, 131.2, 128.5, 128.2, 127.5, 127.0, 126.2, 123.8, 122.2, 121.9 (arom.); 96.1, 86.9 (ethynyl); 31.5, 31.3, 29.6, 29.4, 28. 8, 22.3, 20.1, 19.7, 19.6, 18.2, 18.0, 17.9, 13.6 (aliph.). IR (KBr): $\tilde{\nu}$ = 3443, 2924, 2851, 2208 ($\nu$C≡C), 1589, 1499, 1433, 1253, 1222, 1112, 1023, 841, 777, 723, 558. ESI-MS: calcd. for $C_{114}H_{114}N_8O_{10}Cu_2^{2+}$ [$M^{2+}$]: *m/z* 941.5, found: *m/z* 941.2. $C_{114}H_{118}Cu_2N_8O_{12}\times2PF_6\times2H_2O$ (2209.22): C 61.98, H 5.38, N 5.07; found: C 61.85, H 4.35, N 5.04.

**[$Cu_2$(1a)(4c)$_2$]($PF_6$)$_2$ (R5):** M.p. > 300 °C. $^1$H NMR ($CD_2Cl_2$, 200 MHz): $\delta$ = 8.80 (s, 4 H, phen), 7.93 (s, 2 H, phen), 7.83 (d, 2 H, *J* = 7.9 Hz, phen), 7.61 (dd, *J* = 8.8, *J* = 4.1 Hz, 4 H, phen), 6.85–7.22 (m, 40 H, phen and anthracene), 6.64 (m, 4 H, phen and phenyl), 4.19 (t, *J* = 6.4 Hz, 8 H, -$OCH_2$-), 2.78 (m, 8 H, aliph. and benzyl), 1.24–1.63 (m, 50 H, benzyl), 0.76–0.93 (m, 24 H, aliph.), 0.49 (t, *J* = 5.9 Hz, 12 H, aliph.). $^{13}$C NMR ($CD_2Cl_2$, 100 MHz): $\delta$ = 158.4, 158.4, 154.5, 155.2, 149.1, 147.3, 143.7, 143.1, 141.6, 140.9, 140.4, 139.6, 138.4, 136.6, 135.1, 133.5, 130.4, 129.4, 128.3, 127.4, 126.8, 125.9, 125.3, 124.9, 121.3, 117.5, 114.3, 103.9 (arom.); 91.9, 84.5 (ethynyl); 32.4, 32.3 (2C), 31.1 (2C), 30.1 (2C), 29.2 (2C), 26.5, 23.1 (2C), 22.3 (2C), 14.5, 14.3, 13.8 (2C) (aliph.). IR (KBr): $\tilde{\nu}$ = 3461, 3053, 2923, 2853, 2209 ($\nu$C≡C), 1622, 1604, 1545, 1498, 1461, 1366, 1345, 1276, 1220, 1106, 1014, 958, 841, 791, 736, 723, 557, 532. ESI-MS: calcd. for $C_{162}H_{158}Cl_4Cu_2N_8O_2^{2+}$ [$M^{2+}$]: *m/z* 1258.9, found: *m/z* 1257.9. $C_{162}H_{164}Cl_4Cu_2N_8O_5\times2PF_6\times3H_2O$ (2861.92): C 67.99, H 5.78, N 3.92; found: C 67.54, H 5.32, N 3.85.

**[$Cu_2$(1b)(4a)$_2$]($PF_6$)$_2$ (R6):** M.p. > 300 °C. $^1$H NMR ($CD_2Cl_2$, 400 MHz): $\delta$ = 8.75 (d, *J* = 8.08, 4 H, phen), 8.43–8.52 (m, 8 H, phen), 8.25 (s, 4 H, phen), 7.91 (m, 8 H, phen), 7.75 (q, *J* = 4.8 Hz, 2 H, phen), 7.08 (s, 2 H, phenyl), 4.02 (t, *J* = 6.3 Hz, 4 H, -$OCH_2$-), 2.40 (s, 3 H, benzyl), 1. 95 (s, 3 H, benzyl), 1.77 (s, 16 H, aliph.), 1.65 (s, 12 H, benzyl), 1.53 (s, 12 H, benzyl), 1.45 (s, 6 H, benzyl), 1.41 (m, 6 H, benzyl), 1.20 (m, 6 H, benzyl), 0.71 (t, *J* = 7.08 Hz, 6 H, aliph.). $^{13}$C NMR ($CD_2Cl_2$, 100 MHz): $\delta$ = 159.1, 154.3, 149.0, 148.1, 144.6, 142.4, 141.2, 140.7, 138.7, 138.1, 135.2, 134.6, 133.1, 132.9, 132.5, 129.7, 128.8, 128.1, 127.1, 126.4, 125.2, 121.5, 116.1, 113.2 (arom.); 92.4, 91.1 (ethynyl); 31.2, 29.4, 25.4, 22.1, 21.6, 20.9, 19.6, 14.1 (aliph.). IR (KBr): $\tilde{\nu}$ = 3394, 2921, 2301 ($\nu$C≡C), 1736, 1618, 1495, 1427, 1426, 1368, 1018, 956, 842, 724, 633, 557. ESI-MS: calcd. for $C_{110}H_{102}Br_4Cu_2N_8O_2^{2+}$ [$M^{2+}$]: *m/z* 1007.3, found: *m/z* 1006.2; X-ray structure see Figure 4.

**Crystal Structure Determinations:** Crystals were obtained by slow diffusion of toluene into a solution of the complexes in dichloromethane. Due to the poor quality of the crystals the crystal data are not excellent. Solvent molecules are severely disordered. The measurements were carried out with a STOE-IPDS2 diffractometer with graphite-monochromatised Mo-*Kα* radiation. Table 3 summarises the crystal data, data collection, and refinement parameters. All calculations were performed with the SHELXS-97 package.

Table 3. X-ray experimental data for [$Cu_2$(**2**)$(MeCN)_2\times2PF_6$] and [$Cu_2$(**1b**)(**4a**)$\times2PF_6$].

| Formula | [$Cu_2$(**2**)$(MeCN)_2\times2PF_6$] | [$Cu_2$(**1b**)(**4a**)$_2\times2PF_6$] |
|---|---|---|
| | $C_{76}H_{66}Br_2Cu_2F_{12}N_6P_2$ | $C_{110}H_{102}Br_4Cu_2F_{12}N_8O_2P_2$ |
| $M_w$ | 1640.21 | 2304.68 |
| Crystal system | monoclinic | triclinic |
| Space group | *P*1 21/c 1 (no. 14) | *P*–1 (no. 2) |
| *a* [A°] | 21.297(4) | 13.0625(80) |
| *b* [A°] | 22.658(5) | 21.250(15) |
| *c* [A°] | 17.044(3) | 23.75(2) |
| *α* [°] | 90.00 | 113.00(3) |
| *β* [°] | 104.29(3) | 95.00(3) |
| *γ* [°] | 90.00 | 94.00(3) |
| *V* [$A^3$] | 7970(3) | 6006.46(800) |
| *Z* | 4 | 2 |
| Color | yellow | red |
| Crystal shape | needle | needle |
| Crystal dimensions | 0.3×0.15×0.1 | 0.3×0.15×0.1 |
| $D_{calcd.}$ [$g\,cm^{-3}$] | 1.367 | 1.274 |
| *F*(000) | 3656 | 2656 |
| Radiation | Mo-*Kα*, graphite-monochromated | Mo-*Kα*, graphite-monochromated |
| Device type | IPDS2 STOE | IPDS2 STOE |
| Reflections collected | 44882 | 43551 |
| *R*(int.) | 0.0543 | 0.1144 |
| Independent reflections | 20487 | 22023 |
| Data/parameters | 20487/900 | 22023/1285 |
| GOF on $F^2$ | 1.564 | 1.234 |
| Rreflections threshold expression | $>2\sigma(I)$ | $>2\sigma(I)$ |
| *hkl* limits (max./min.) | –23/29, –26/31, –23/21 | –16/16, –26/26, –29/29 |
| Final *R* indices [$I > 2\sigma(I)$] | $R_1$ = 0.0919, $_wR_2$ = 0.2404 | $R_1$ = 0.1281, $_wR_2$ = 0.2960 |
| *R* indices (all data) | $R_1$ = 0.1259, $_wR_2$ = 0.2558 | $R_1$ = 0.2317, $_wR_2$ = 0.3352 |

  

## Acknowledgments

We would like to express our gratitude to the Deutsche Forschungsgemeinschaft (Schm 647/12-1 and -/13-1) and the Fonds der Chemischen Industrie for financial support.

[1] a) H. Sleiman, P. Baxter, J.-M. Lehn, K. Rissanen, *J. Chem. Soc. Chem. Commun.* **1995**, 715–716; b) G. S. Hanan, C. R. Arana, J.-M. Lehn, G. Baum, D. Fenske, *Angew. Chem. Int. Ed. Engl.* **1995**, *34*, 1122–1124; c) G. S. Hanan, C. R. Arana, J.-M. Lehn, G. Baum, D. Fenske, *Chem. Eur. J.* **1996**, *2*, 1292–1302; d) H. Sleiman, P. N. W. Baxter, J.-M. Lehn, K. Airola, K. Rissanen, *Inorg. Chem.* **1997**, *36*, 4734–4742; e) D. Brown, R. Zong, R. P. Thummel, *Eur. J. Inorg. Chem.* **2004**, 3269–3272; f) M. Benaglia, F. Ponzini, C. R. Woods, J. S. Siegel, *Org. Lett.* **2001**, *3*, 967–969; g) P. Ceroni, A. Credi, V. Balzani, S. Campagna, G. S. Hanan, C. R. Arana, J.-M. Lehn, *Eur. J. Inorg. Chem.* **1999**, 1409–1414.

[2] M. Schmittel, V. Kalsani, *Top. Curr. Chem.* **2004**, *245*, 1–53.

[3] a) U. Drechsler, B. Erdogan, V. M. Rotello, *Chem. Eur. J.* **2004**, *10*, 5570–5579; b) P. H. Kwan, M. J. MacLachlan, T. M. Swager, *J. Am. Chem. Soc.* **2004**, *126*, 8638–8639.

[4] a) C. O. Dietrich-Buchecker, J. P. Sauvage, J. P. Kintzinger, *Tetrahedron Lett.* **1983**, *24*, 5095–5098; b) U. Velten, M. Rehahn, *Chem. Commun.* **1996**, 2639–2640; c) S. S. Zhu, P. J. Carroll, T. M. Swager, *J. Am. Chem. Soc.* **1996**, *118*, 8713–8714.

[5] The HETPHEN (**het**eroleptic bis**phen**anthroline) approach is based on steric and electronic effects originating from bulky aryl substituents at the bisimine coordination sites to control the coordination equilibrium both kinetically and thermodynamically.

[6] a) V. Kalsani, H. Ammon, F. Jäckel, J. P. Rabe, M. Schmittel, *Chem. Eur. J.* **2004**, *10*, 5481–5492; b) M. Schmittel, V. Kalsani, L. Kienle, *Chem. Commun.* **2004**, 1534–1535; c) M. Schmittel, A. Ganz, D. Fenske, *Org. Lett.* **2002**, *4*, 2289–2292; d) M. Schmittel, H. Ammon, V. Kalsani, A. Wiegrefe, C. Michel, *Chem. Commun.* **2002**, 2566–2567.

[7] a) A. Marquis-Rigault, A. Dupont-Gervais, P. N. W. Baxter, A. Van Dorsselaer, J.-M. Lehn, *Inorg. Chem.* **1996**, *35*, 2307–2310; b) P. N. W. Baxter, J.-M. Lehn, B. O. Kneisel, G. Baum, D. Fenske, *Chem. Eur. J.* **1999**, *5*, 113–120; c) A. M. Garcia, D. M. Bassani, J.-M. Lehn, G. Baum, D. Fenske, *Chem. Eur. J.* **1999**, *5*, 1234–1238; d) P. N. W. Baxter, J.-M. Lehn, B. O. Kneisel, D. Fenske, *Angew. Chem. Int. Ed. Engl.* **1997**, *36*, 1978–1981.

[8] M. Schmittel, V. Kalsani, D. Fenske, A. Wiegrefe, *Chem. Commun.* **2004**, 490–491.

[9] a) M. Schmittel, A. Ganz, *Chem. Commun.* **1997**, 999–1000; b) M. Schmittel, U. Lüning, M. Meder, A. Ganz, C. Michel, M. Herderich, *Heterocycl. Commun*. 1997, **3**, 493–494.

[10] M. Schmittel, V. Kalsani, unpublished results.

[11] M. Schmittel, C. Michel, A. Wiegrefe, V. Kalsani, *Synthesis* **2001**, 1561–1567.

[12] U. Lüning, M. Müller, *Chem. Ber.* **1990**, *123*, 643–645.

[13] M. Schmittel, C. Michel, S. X. Liu, D. Schildbach, D. Fenske, *Eur. J. Inorg. Chem.* **2002**, 1155–1166.

[14] a) H. Gampp, M. Maeder, C. J. Meyer, A. D. Zuberbühler, *Talanta* **1985**, *32*, 95–101; b) F. J. C. Rossotti, H. S. Rossotti, R. J. Whewell, *J. Inorg. Nucl. Chem.* **1971**, *33*, 2051–2065; c) H. Gampp, M. Maeder, C. J. Meyer, A. D. Zuberbühler, *Talanta* **1985**, *32*, 257–264; d) H. Gampp, M. Maeder, C. J. Meyer, A. D. Zuberbühler, *Talanta* **1986**, *33*, 943–951.

[15] I. Higler, L. Grave, E. Breuning, W. Verboom, F. D. Jong, T. M. Fyles, D. N. Reinhoudt, *Eur. J. Org. Chem.* **2000**, 1727–1734.

[16] a) P. N. W. Baxter, *Comprehensive, supramolecular chemistry* (Eds.: J. L. Atwood, J. E. D. Davies, D. D. MacNicol, F. Vögtle, J.-M. Lehn), Pergamon, Oxford, **1996**, vol. 9, chapter *5*, 165–211; b) L. J. Charbonnière, A. F. Williams, U. Frey, A. E. Merbach, P. Kamalaprija, O. Schaad, *J. Am. Chem. Soc.* **1997**, *119*, 2488–2496; c) B. Olenyuk, A. Fechtenkotter, P. J. Stang, *J. Chem. Soc. Dalton Trans.* **1998**, *11*, 1707–1728; d) S. Leininger, B. Olenyuk, P. J. Stang, *Chem. Rev.* **2000**, *100*, 853–907; e) C. Addicott, N. Das, P. J. Stang, *Inorg. Chem.* **2004**, *43*, 5335–5338; f) F. Würthner, A. Sautter, D. Schmid, P. J. A. Weber, *Chem. Eur. J.* **2001**, *7*, 894–902; g) S. Hiraoka, Y. Kubota, M. Fujita, *Chem. Commun.* **2000**, 1509–1510.

[17] N. Armaroli, *Chem. Soc. Rev.* **2001**, *30*, 113–124.

Received: October 25, 2004

  